

# Formation of textures and microstructures in asymmetrically cold rolled and subsequently annealed aluminum alloy 1100 sheets

JONG-KOOK KIM, YOUNG-KYU JEE, MOO-YOUNG HUH\*

*Division of Materials Science and Engineering, Korea University, Seoul 136-701, Korea*  
E-mail: myhuh@korea.ac.kr

HYO-TAE JEONG

*Department of Metallurgical Engineering, Kangnung University, Kangnung 210-702, Korea*

The formation of textures and microstructures in asymmetrically cold rolled and subsequently annealed AA 1100 sheets was investigated. The asymmetrical rolling procedure in this experiment was performed in a rolling mill with different roll velocities (roll velocity ratio of 1.5/1.0). In order to enhance the shear deformation, asymmetrical rolling was performed by a large reduction per pass and without lubrication. Asymmetrical rolling led to the formation of strong shear textures. The evolution of asymmetrically cold rolled textures was analyzed by FEM simulations. After recrystallization annealing, pronounced  $\{111\}$ //ND orientations prevailed in all thickness layers. Intensified shear deformations by asymmetrical rolling also led to the formation of ultra-fine grains after recrystallization annealing. © 2004 Kluwer Academic Publishers

## 1. Introduction

During normal symmetrical rolling factors like geometrical changes during a rolling pass and friction between roll and sheet surface may cause deviations from the ideal plane strain condition. However, the strain state accompanying symmetrical rolling deformation is commonly simplified by a plane strain state (e.g. [1, 2]). The texture in normally cold rolled aluminum mainly comprises orientations that are typical of plane strain deformation of fcc metals and alloys. In such textures, most orientations are assembled along the so-called  $\beta$ -fiber, that runs through the Euler angle space from the  $C$ -orientation  $\{112\}\langle 111 \rangle$  through the  $S$ -orientation  $\{123\}\langle 634 \rangle$  to the  $B$ -orientation  $\{011\}\langle 211 \rangle$  (e.g. [3]).

Rolling with different angular speeds or different roll diameters gives rise to the asymmetrical strain state in the roll gap. Asymmetrical rolling is one of the most effect ways to obtain shear textures [4, 5]. Typical shear texture components of aluminum strips are the  $45^\circ$  ND rotated cube-orientation  $\{001\}\langle 110 \rangle$  and  $\{111\}\langle uvw \rangle$  orientations. Note that  $\{111\}\langle uvw \rangle$  orientations are beneficial for improving the deep drawability [6]. Recently, Kim and his coworkers [7] reported that fine-grained aluminum sheets can be produced by means of asymmetrical rolling. Our recent work [8] disclosed the formation of ultra-fine grains during the normal symmetrical rolling deformation with a large reduction per rolling pass.

In the present work, asymmetrical rolling was performed by a large reduction per pass and without lu-

brication in order to maximize the shear deformation. The formation of through-thickness textures and microstructures in asymmetrically cold rolled and subsequently annealed AA 1100 sheets was investigated. The strain states during asymmetrical rolling were analyzed by the finite element method (FEM).

## 2. Experimental procedure

The initial material was 4.0 mm thick, cold rolled strip of the commercial aluminum alloy 1100. The sample was asymmetrically cold rolled using a laboratory rolling mill with a roll diameter of 128 mm in a single pass to the final thickness of 1.5 mm. The asymmetrical rolling was performed with a roll speed ratio of 1.5/1.0 (18 and 12 rotations/min for upper and low roll, respectively). The asymmetrical rolling was carried out without lubrication in order to maximize shear deformation. The asymmetrically rolled sheets were finally subjected to a recrystallization annealing for about 1 h at  $300^\circ\text{C}$ . Various through-thickness layers of the sheets were prepared by careful grinding, polishing and etching of the sheets down to the layer of interest. In the following, the sheet layers are indicated by the parameter  $s$ , with  $s = 0.0$ ,  $s = +1.0$  and  $s = -1.0$  denoting the center, upper surface and lower surface of the sheets, respectively.

For texture analysis pole figures were measured at different layers of the sheets by means of a conventional X-ray texture goniometer [9]. From three incomplete

\*Author to whom all correspondence should be addressed.

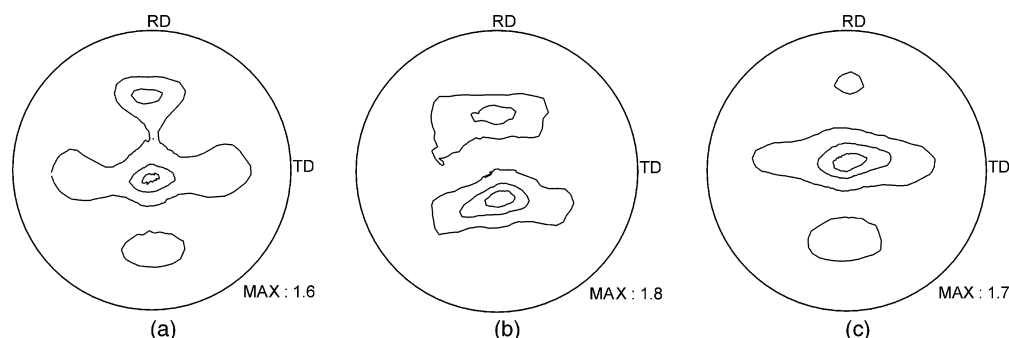


Figure 1 {111} pole figures showing through-thickness textures in AA 1100 after asymmetrical rolling.

pole figures, the three-dimensional orientation distribution functions (ODF)  $f(g)$  were calculated by the series expansion method ( $l_{\max} = 22$ ) proposed by Bunge [10]. After asymmetrical rolling, most of the pole figures displayed the typical monoclinic sample symmetry; accordingly, the ODFs were calculated in the Euler angle range of  $\{0^\circ \leq \varphi_1 \leq 180^\circ, 0^\circ \leq \Phi, \varphi_2 \leq 90^\circ\}$ .

### 3. Results and discussion

Some texture gradients throughout thickness layers were found in the initial sample. However, the initial sample displayed the typical cold rolling texture of aluminum alloy in whole thickness layers. Asymmetrical rolling with a large reduction in a single pass from 4 to 1.5 mm led to a pronounced change in textures as shown in Fig. 1. In the upper surface ( $s = +1.0$ ) in contact with fast upper roll, typical shear textures of fcc metals were found (Fig. 1a). The maximum texture intensity was obtained in the  $45^\circ$  ND rotated cube orientation  $\{001\}\langle 110 \rangle$  and pronounced ND-scatters of  $\{001\}\langle 100 \rangle$  and  $\{111\}\langle uvw \rangle$  orientations were also observed. The similar texture was observed in the lower surface ( $s = -1.0$ ) in contact with slow lower roll ( $s = -1.0$ ). Here, the intensity of  $\{111\}\langle uvw \rangle$  orientations was much higher than  $s = +1.0$ . It was noted that the textures observed in  $s = +0.5$  and  $-0.5$  were also similar to that found in surfaces. In contrast to other

thickness layers, the center layer ( $s = 0.0$ ) displayed a random texture with weak scattering of  $\{001\}\langle ND \rangle$  orientations (Fig. 1b).

In order to investigate the evolution of shear textures more precisely, three dimensional orientation distribution functions were calculated [10]. As an example, Fig. 2 shows ODF of the lower surface ( $s = -1.0$ ) in contact with slow lower roll. Because of monoclinic sample symmetry, ODFs were calculated in the Euler angle range of  $\{0^\circ \leq \varphi_1 \leq 180^\circ, 0^\circ \leq \Phi, \varphi_2 \leq 90^\circ\}$ . The lower surface layer ( $s = -1.0$ ) displays the maximum intensity at  $(90^\circ, 20^\circ, 45^\circ)$  and strong  $\{001\}\langle 110 \rangle$  and  $\{111\}\langle uvw \rangle$ . Interestingly,  $\{111\}\langle uvw \rangle$  orientations form a  $\gamma$ -fiber in the orientation space along  $\varphi_1$  angles with  $\Phi = 55^\circ$  in  $\varphi_2 = 45^\circ$  section.

The evolution of crystallographic textures depends on the strain state during the plastic deformation. In order to tackle the strain state, the present process of asymmetrical rolling was analyzed with the two-dimensional FEM. Because of the two-dimensional analysis, deviation from the ideal plane strain condition is manifested in a non-zero strain rate component  $\dot{\epsilon}_{13}$ . Fig. 3 shows the variation of the shear strain state in AA 1100 sheet during asymmetrical rolling calculated by FEM. Friction coefficient  $\mu = 0.2$  between roll and sample were assumed for the FEM simulations. The shear strain rate  $\dot{\epsilon}_{13}$  in the rolling gap is not homogeneous but varies throughout the thickness,

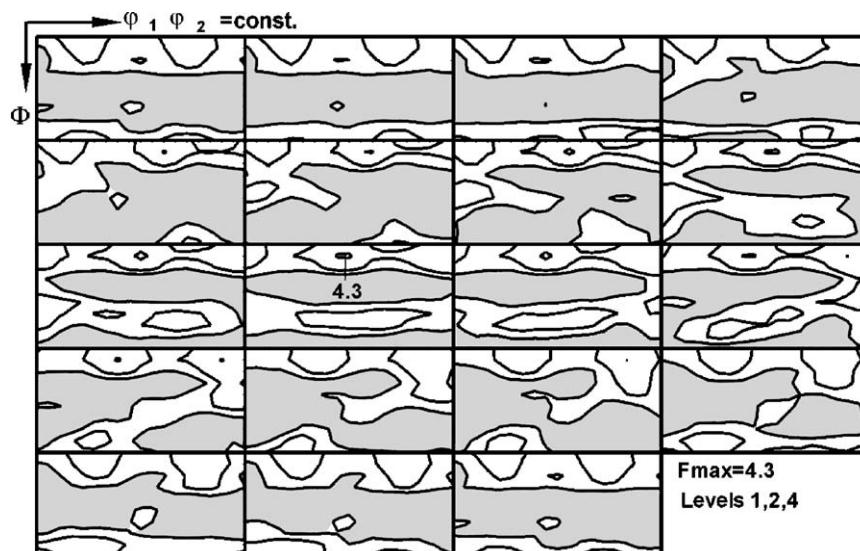


Figure 2 Three dimensional ODF showing textures of  $s = -1.0$ .

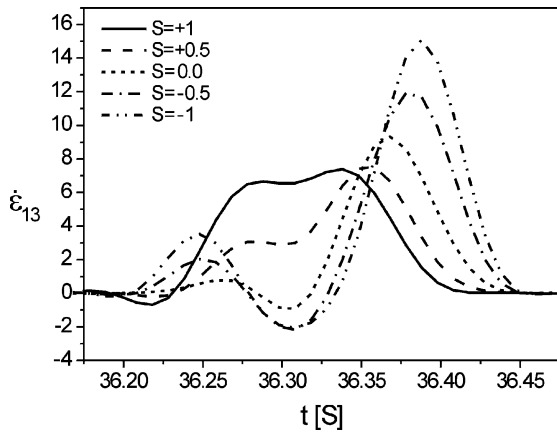


Figure 3 Variation of shear strain rate  $\epsilon_{13}$  in a roll gap during asymmetrical rolling.

TABLE I Integrated strain components in a roll gap

Thickness layer	$\epsilon_{11}$	$ \epsilon_{13}^{Pos} $	$ \epsilon_{13}^{Neg} $	$( \epsilon_{13}^{Pos}  +  \epsilon_{13}^{Neg} )/\epsilon_{11}$
$s = +1.0$	1.17	1.08	0.03	0.95
$s = +0.5$	1.10	0.92	0.01	0.84
$s = 0.0$	1.00	0.68	0.01	0.69
$s = -0.5$	0.98	0.76	0.03	0.81
$s = -1.0$	0.97	0.84	0.07	0.94

which leads to the evolution of texture gradients. In the literatures [1, 11], the ratio of shear strain to normal strain ( $\epsilon_{13}/\epsilon_{11}$ ) can be a criterion for the formation of shear or plane strain textures. The present FEM result is summarized in Table I.  $|\epsilon_{13}^{Pos}|$  and  $|\epsilon_{13}^{Neg}|$  denote absolute values of integrated shear strain rates for positive and negative  $\epsilon_{13}$ , respectively. It appears that shear textures developed in the thickness layers having the stain state  $(|\epsilon_{13}^{Pos}| + |\epsilon_{13}^{Neg}|)/\epsilon_{11} > 0.8$ . Unlike to other thickness

layers, the center layer ( $s = 0.0$ ) displayed a random texture with weak scattering of  $\{001\}$ //ND orientations. Note that  $(|\epsilon_{13}^{Pos}| + |\epsilon_{13}^{Neg}|)/\epsilon_{11}$  in  $s = 0.0$  is smaller than 0.7.

$\{111\}$  pole figures in Fig. 4 show through-thickness textures of the recrystallized sample. In general, the texture features of asymmetrically cold rolled samples were largely retained after recrystallization annealing at 300°C for 1 h. Whereas the overall texture intensity of the center layer ( $s = 0.0$ ) slightly decreases, the recrystallization leads to an increase in the texture intensity of the upper and lower surface layers ( $s = +1.0$  and  $-1.0$ ). Note that the intensity of the desired  $\{111\}\langle uvw \rangle$  orientations significantly increased to the detriment of  $\{001\}\langle 110 \rangle$  in surface layers. Fig. 5 shows ODF of lower surface layer ( $s = -1.0$ ). Evidently,  $\{111\}\langle uvw \rangle$  orientations prevail and  $\{001\}\langle uvw \rangle$  orientations markedly

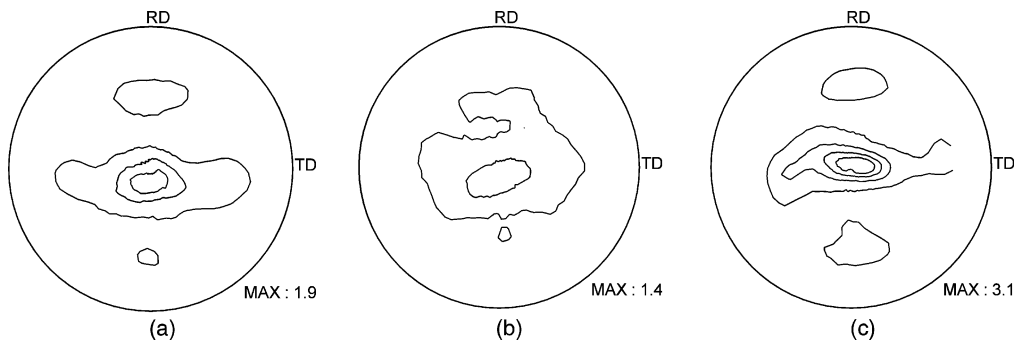


Figure 4  $\{111\}$  pole figures showing recrystallization textures in AA 1100 after asymmetrical rolling.

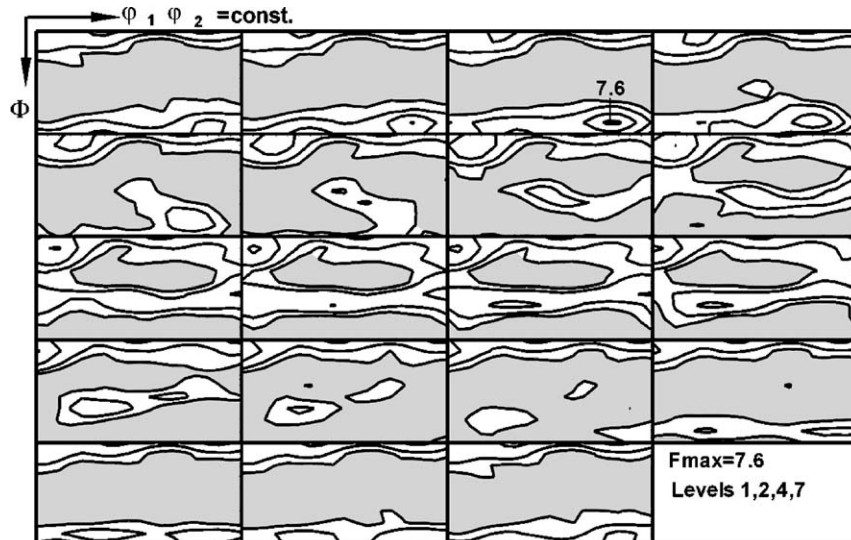


Figure 5 Three dimensional ODF showing recrystallization texture of  $s = -1.0$ .

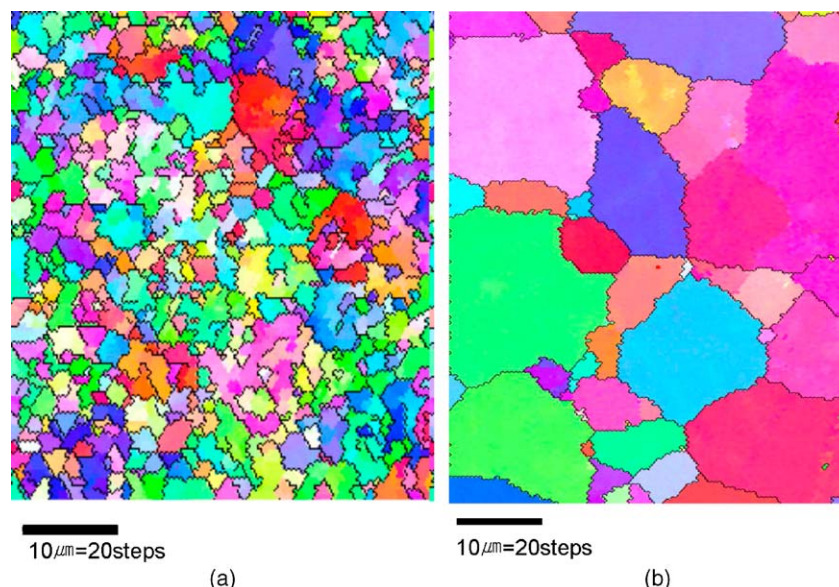


Figure 6 EBSD after recrystallization annealing at 300°C for 1 h observed from (a) surface layer and (b) center layer.

decrease after recrystallization annealing at 300°C for 1 h.

As mentioned previously, the strain state accompanying symmetrical rolling deformation is commonly simplified by a plane strain state (e.g. [1, 2]). In Al-alloys deformed under plane strain conditions, recrystallization is dominated by the abundant existence of deformation heterogeneities that may act as nucleation sites—in particular cube-bands, grain boundaries and, if present, second-phase particles and shear bands (e.g. [12, 13]). In the asymmetrically rolled sheets, in contrast, the conditions are obviously unfavourable for forming and/or sustaining cube-bands.

In the literature on recrystallization textures it is commonly assumed that the stored energy of the various texture components is proportional to their Taylor-factor,  $M$  (e.g. [14]). Among the shear texture orientations,  $\{001\}\langle 110 \rangle$  has the lowest Taylor-factor and  $\{111\}\langle uvw \rangle$  orientations have Taylor-factors of the order of  $M \approx 3.0$  [14]. Thus, nucleation of grains with  $\{111\}\langle uvw \rangle$  orientations should be facilitated. Accordingly, strong increase in  $\{111\}\langle uvw \rangle$  orientations in the final recrystallization texture of asymmetrically rolled samples is attributed to favourable nucleation in  $\{111\}\langle uvw \rangle$  orientations.

Fig. 6 shows examples of recrystallized microstructures observed by electron back scattered diffraction (EBSD). Grain boundary having misorientation larger than 15° was indicated with lines in Fig. 6. It was noted that the thickness layers depicting pronounced  $\{111\}\langle uvw \rangle$  orientations display fine grains smaller than 3.0 μm. In contrast, the center layer having a random recrystallization texture reveals grains larger than 10 μm. Severe shear deformations including equal angular channel pressing (ECAP), continuous confined strip shearing (CCSS) and torsion straining give rise to the formation of fine grains (e.g. [15, 16]). Accordingly, it is concluded that asymmetrical rolling with a large reduction per a rolling pass and without lubrication in the present experiment intensified shear deformations in

the sample, which led to the evolution of shear textures and fine grains.

#### 4. Summary

Asymmetrical rolling was performed by a large reduction per pass and without lubrication in order to maximize the shear deformation. The center layer ( $s = 0.0$ ) displayed a random texture with weak scattering of  $\{001\}$ //ND orientations. In other thickness layers including upper and lower surfaces, typical shear textures of fcc metals were found. The ratio of shear strain to normal strain ( $\varepsilon_{13}/\varepsilon_{11}$ ) is a measure for the evolution of shear or plane strain textures. Strong increase in  $\{111\}\langle uvw \rangle$  orientations in the final recrystallization texture of asymmetrically rolled samples is attributed to favorable nucleation in  $\{111\}\langle uvw \rangle$  orientations. Intensified shear deformations by asymmetrical rolling led to the formation of fine grains after recrystallization annealing.

#### Acknowledgements

This work was supported by grant No. R01-2001-000-00261-0 from the Korean Science and Engineering Foundation.

#### References

1. O. ENGLER, M. Y. HUH and C. N. TOME, *Metall. Mater. Trans. A* **31** (2000) 2299.
2. C. S. LEE and B. J. DUGGAN, *Metall. Trans. A* **22** (1991) 2637.
3. J. HIRSCH and K. LÜCKE, *Acta Metall.* **36** (1988) 2883.
4. K. H. KIM and D. N. LEE, *Acta Mater.* **49** (2001) 2583.
5. S. H. LEE and D. N. LEE, *Inter. J. Mech. Sci.* **43** (2001) 1997.
6. P. H. LEQUEU and J. J. JONAS, *Metall. Trans. A* **19** (1988) 105.
7. S. H. KIM, J. H. RYU, K. H. KIM and D. N. LEE, *Mater. Sci. Res. Inter.* **8** (2002) 20.
8. M. Y. HUH, H. D. KIM, K. R. LEE, B. B. HWANG and O. ENGLER, *Mater. Sci. Forum* **408–412** (2002) 1453.

## MECHANOCHEMISTRY AND MECHANICAL ALLOYING 2003

9. V. RANDLE and O. ENGLER, "Introduction to Texture Analysis, Macrotexture, Microtexture and Orientation Mapping" (Gordon and Breach, Amsterdam, 2000).
10. H. J. BUNGE, "Texture Analysis in Materials Science" (Butterworths, London, 1982).
11. M. Y. HUH, J. C. LEE and S. LEE, *Met. Mater. Inter.* **2** (1996) 141.
12. D. JUUL JENSEN, N. HANSEN and F. J. HUMPHREYS, *Acta Metall.* **33** (1985) 2155.
13. O. ENGLER, *Mater. Sci. Technol.* **12** (1996) 859.
14. O. ENGLER, H. C. KIM and M. Y. HUH, *ibid.* **17** (2001) 75.
15. V. M. SEGAL, *Mater. Sci. Eng.* **197A** (1995) 157.
16. R. Z. VALIEV, A. V. KORZNIKOV and R. R. MULYUKOV, *ibid.* **168A** (1993) 141.

*Received 11 September 2003  
and accepted 27 February 2004*